

The Differential Interactions of Peroxisome Proliferator-Activated Receptor γ Ligands with Tyr473 Is a Physical Basis for Their Unique Biological Activities

Monica Einstein, Taro E. Akiyama, Gino A. Castriota, Chuanlin F. Wang, Brian McKeever,¹ Ralph T. Mosley,² Joseph W. Becker, David E. Moller,³ Peter T. Meinke, Harold B. Wood, and Joel P. Berger

Departments of Metabolic Disorders (M.E., T.E.A., G.A.C., C.F.W., D.E.M., J.P.B.) and Medicinal Chemistry (B.M., R.T.M., J.W.B., P.T.M., H.B.W.), Merck Research Laboratories, Rahway, New Jersey

Received August 29, 2007; accepted October 16, 2007

ABSTRACT

Despite their proven antidiabetic efficacy, widespread use of peroxisome proliferator-activated receptor (PPAR) γ agonists has been limited by adverse cardiovascular effects. To overcome this shortcoming, selective PPAR γ modulators (SPPAR γ M) have been identified that have antidiabetic efficacy comparable with full agonists with improved tolerability in preclinical species. The results of structural studies support the proposition that SPPAR γ M interact with PPAR γ differently from full agonists, thereby providing a physical basis for their novel activities. Herein, we describe a novel PPAR γ ligand, SPPAR γ M2. This compound was a partial agonist in a cell-based transcriptional activity assay, with diminished adipogenic activity and an attenuated gene signature in cultured human adipocytes. X-ray cocrystallography studies demonstrated that, unlike rosiglitazone, SPPAR γ M2 did not interact

with the Tyr473 residue located within helix 12 of the ligand binding domain (LBD). Instead, SPPAR γ M2 was found to bind to and activate human PPAR γ in which the Tyr473 residue had been mutated to alanine (hPPAR γ Y473A), with potencies similar to those observed with the wild-type receptor (hPPAR γ WT). In additional studies, we found that the intrinsic binding and functional potencies of structurally distinct SPPAR γ M were not diminished by the Y473A mutation, whereas those of various thiazolidinedione (TZD) and non-TZD PPAR γ full agonists were reduced in a correlative manner. These results directly demonstrate the important role of Tyr473 in mediating the interaction of full agonists but not SPPAR γ M with the PPAR γ LBD, thereby providing a precise molecular determinant for their differing pharmacologies.

Use of Industrial Macromolecular Crystallography Association Collaborative Access Team beamline 17-ID (or 17-BM) at the Advanced Photon Source was supported by the companies of the Industrial Macromolecular Crystallography Association through a contract with the Center for Advanced Radiation Sources at the University of Chicago (Chicago, IL). All work presented here was performed by employees of Merck and Co. and was completely funded by Merck and Co.

M.E. and T.E.A. contributed equally to the research communicated in this article.

¹ Current affiliation: Vitae Pharmaceuticals, Inc., Fort Washington, Pennsylvania.

² Current affiliation: Pharmasset, Inc., Princeton, New Jersey.

³ Current affiliation: Lilly Research Laboratories, Indianapolis, Indiana.

Article, publication date, and citation information can be found at <http://molpharm.aspetjournals.org>.

doi:10.1124/mol.107.041202.

The peroxisome proliferator-activated receptors (PPARs) γ , δ , and α compose a nuclear receptor subfamily that modulates the transcription of a large compendium of genes encoding proteins that regulate lipid metabolism, cell differentiation, and signal transduction in a ligand-dependent manner (Berger and Moller, 2002). PPAR γ has been shown to be a master regulator of adipogenesis and nutrient metabolism in adipocytes where it is highly expressed. Thiazolidinedione (TZD) PPAR γ full agonists have demonstrated clinical efficacy for the treatment of type 2 diabetes mellitus (T2DM) patients (Berger et al., 2005). However, the use of these insulin-sensitizing agents has been restricted because of their association with several adverse effects, including

ABBREVIATIONS: PPAR, peroxisome proliferator-activated receptor; TZD, thiazolidinedione; SPPAR γ M, selective peroxisome proliferator-activated receptor γ modulator; T2DM, type 2 diabetes mellitus; LBD, ligand binding domain; WT, wild type; GST, glutathione transferase; PCR, polymerase chain reaction; nTZDpa, nonthiazolidinedione-selective peroxisome proliferator-activated receptor γ modulator; FABP4, fatty acid-binding protein 4; PEPCK, phosphoenolpyruvate carboxykinase; ADFP, adipose differentiation-related protein; FK-614, 3-(2,4-dichlorobenzyl)-2-methyl-N-(pentylsulfonyl)-3H-benzimidazole-5-carboxamide; GI262570, (2S)-2-[[2-(benzoyl)phenyl]amino]-3-[4-[2-(5-methyl-2-phenyl-1,3-oxazol-4-yl)ethoxy]phenyl]propanoic acid; GW0072, 4-[4-[(2S,5S)-5-[2-(bis(phenylmethyl)amino)-2-oxoethyl]-2-heptyl-4-oxo-1,3-thiazolidin-3-yl]butyl]benzoic acid; PA-082, 1-(3,4-dimethoxy-benzyl)-6,7-dimethoxy-4-[4-(2-methoxy-phenyl)-piperidin-1-ylmethyl]-isoquinoline.

plasma volume expansion and edema that can cause or exacerbate congestive heart failure, as well as weight gain, which seems to result from both increased adiposity and plasma volume. Thus, there exists a critical need to develop PPAR γ -targeted insulin-sensitizing agents that display robust antidiabetic efficacy with improved tolerability.

To meet this challenge, we and others have identified and characterized promising selective PPAR γ modulators (SPPAR γ M_s). SPPAR γ M_s are PPAR γ ligands that serve as partial agonists of the receptor in cell-based transcriptional activity and adipogenesis assays (Berger et al., 2005). They have also been shown to generate attenuated gene signatures in rodent adipocytes in vitro and adipose tissue in vivo. The superior therapeutic window of several SPPAR γ M_s has been established in preclinical species. For example, nTZDpa demonstrated robust insulin-sensitizing activity in obese C57/BL6 mice with attenuated adverse effects on weight gain, adiposity, and cardiac hypertrophy relative to a potent PPAR γ full agonist (Berger et al., 2003). Compounds 24 (Acton et al., 2005) and 5 (Dropinski et al., 2005) are structurally unique SPPAR γ M_s that demonstrated antihyperglycemic efficacy comparable with rosiglitazone in diabetic db/db mice with reduced weight gain at similar plasma exposures. The SPPAR γ M FK614 has been shown to have significant antidiabetic activity in mice with diminished hemodilution and cardiac hypertrophy in rats (Minoura et al., 2004). Remarkably, the angiotensin receptor blocker telmisartan exhibited SPPAR γ M activity, including robust amelioration in insulin resistance in diet-induced obese mice without increasing weight gain (Schupp et al., 2005). A novel SPPAR γ M, PA-082, has been described that, compared with PPAR γ full agonists, has a diminished ability to induce lipid accumulation during in vitro adipogenesis of preadipocytes but maintains the ability to ameliorate cytokine-induced insulin resistance in cultured adipocytes to a similar extent (Burgermeister et al., 2006).

Previously published data seem to indicate that the unique properties of the SPPAR γ M_s may be due to their distinct physical interaction with the receptor, resulting in diminished conformational stability of the receptor compared with full agonists. Indeed, X-ray cocrystallographic studies of the PPAR γ ligand binding domain (LBD) complexed with the full agonist rosiglitazone indicated that the negatively charged nitrogen of the TZD ring of rosiglitazone was within hydrogen-bonding distance of the tyrosine (Y) 473 side-chain hydroxyl group in helix 12 of the human PPAR γ LBD (Nolte et al., 1998). In contrast, X-ray cocrystallography and molecular modeling studies performed with the PPAR γ LBD and SPPAR γ M_s (Oberfield et al., 1999; Burgermeister et al., 2006) indicate that the carboxylic acid moiety of such ligands was not within hydrogen-bonding distance of Tyr473. Consonant with their different binding modes, biochemical and NMR studies have demonstrated that SPPAR γ M_s induce a unique and less stable receptor conformation than PPAR γ full agonists (Berger et al., 2003). Taken together, these studies suggest that Tyr473 is a critical site of interaction between the PPAR γ LBD and full agonists but not SPPAR γ M_s. Thus, Tyr473 is implicated as having an important role in the stabilization of the LBD of the receptor by the former but not the latter class of ligands. Furthermore, because Tyr473 lies within the helix 12 transcriptional activa-

tion function-2 domain that composes a section of the transcriptional coactivator binding pocket of LBD (Nolte et al., 1998; Sheu et al., 2005), the inability of SPPAR γ M_s to bind to and thereby directly stabilize this region may serve as the physical basis for the differential receptor-coactivator interactions, attenuated transcriptional activity, and resulting improved tolerability observed in preclinical species with these ligands (Kintscher et al., 2000; Berger et al., 2003; Minoura et al., 2004; Acton et al., 2005; Dropinski et al., 2005; Schupp et al., 2005).

Here, we describe a novel, potent PPAR γ ligand, SPPAR γ M₂. We found that in comparison with rosiglitazone, SPPAR γ M₂ served as a partial agonist of human PPAR γ in a cell-based transcriptional activity assay, had a diminished ability to induce adipogenesis and triglyceride accumulation in primary cultures of human preadipocytes, and generated an attenuated gene signature in human adipocytes. X-ray cocrystallography studies localized the bound ligand at a considerable distance from the Tyr473 residue within the LBD of the receptor. It is noteworthy that neither the binding nor the transcriptional activity of SPPAR γ M₂ was significantly affected when it was assayed with a mutant PPAR γ in which the Tyr473 residue was changed to an alanine (hPPAR γ Y473A). In additional studies, we found that the Tyr473A mutation did not reduce the binding or transcriptional activities of a structurally diverse cohort of SPPAR γ M_s. In contrast, the intrinsic and functional potencies of various TZD and non-TZD PPAR γ full agonists were significantly reduced in a correlative manner.

Materials and Methods

Site-Directed Mutagenesis and Protein Purification. Generation of the chimeric receptor hPPAR γ Y473A/GAL4 was performed using the previously described mammalian expression plasmid containing the wild-type (WT) human PPAR γ LBD, pcDNA3-hPPAR γ /GAL4 (Elbrecht et al., 1999), oligonucleotides GCTCCTGCAGGAGATCGCCAAGGACTTGTACTAG and CTAGTACAAGTCCCTTGGCGATCTCCTGCAGGAGC, and the QuikChange site-directed mutagenesis kit (Stratagene, La Jolla, CA) to produce the vector pcDNA3-hPPAR γ Y473A/GAL4. GST fusion protein constructs containing the hPPAR γ WT or hPPAR γ Y473A LBD were generated by transferring the nucleotide fragments encoding amino acids 176 to 477 from the above-mentioned pcDNA constructs into a similarly cleaved pGEX-5X-2 vector (GE Healthcare, Chalfont St. Giles, UK). The fusion proteins were then expressed in *Escherichia coli* bacteria and purified on a glutathione-Sepharose column as described previously (Berger et al., 2003).

SPA Binding Assays. A previously described competition binding assay using GST-hPPAR γ and the radioligand [³H]₂nTZD3 (Berger et al., 2003) was used to identify a series of structurally distinct PPAR γ ligands. To compare the potencies of PPAR γ ligands on the wild-type and Y473A mutant PPAR γ , novel competition binding assays using [³H]SPPAR γ M₁ were developed and performed using modified versions of previously described protocols (Berger et al., 2003). To characterize the binding activity of radiolabeled SPPAR γ M₁, saturation binding assays were performed using recombinant GST-hPPAR γ WT LBD or GST-hPPAR γ Y473A LBD, anti-GST antibody (GE Healthcare), and radioligand [³H]SPPAR γ M₁ at 0 to 30 nM \pm 50 μ M nonradioactive SPPAR γ M₁ combined in the same assay buffer and assayed under similar conditions as described previously (Berger et al., 2003). Specific binding was determined from the difference between the total and nonspecific binding. The K_d value was derived from nonlinear regression analysis using the one-site binding equation in Prism (GraphPad Software Inc., San Diego, CA). Subsequently, competition binding assays were per-

formed using recombinant GST-hPPAR γ WT LBD or GST-hPPAR γ Y473A LBD, anti-GST antibody (GE Healthcare), and 2.5 nM [3 H]SPPAR γ M1 in the same buffers and under the same conditions as the aforementioned assays.

Cell Culture and Transient Transactivation Assay. COS-1 cells were cultured and maintained as described previously (Berger et al., 1999). Cells were transfected with the pcDNA3-hPPAR γ WT/GAL4 or pcDNA3-hPPAR γ Y473A/GAL4 expression vector, pUAS(5X)-tk-luc reporter vector, and pCMV-lacZ (as an internal control for transactivation efficiency) using Lipofectamine (Invitrogen, Carlsbad, CA). After a 48-h exposure to compounds, cell lysates were produced, and luciferase and β -galactosidase activity in cell extracts was determined. Inflection points of normalized luciferase activity were calculated by a four-parameter logistic equation in Prism (GraphPad Software Inc.).

Adipogenic Differentiation of Primary Human Preadipocytes. Primary human preadipocytes derived from subcutaneous adipose depots (Zen-Bio, Inc., Research Triangle Park, NC) were differentiated by adding 10 μ M rosiglitazone or SPPAR γ M2 in a final concentration of 0.1% dimethyl sulfoxide in differentiation media (Zen-Bio, Inc.) for 5 days. The media were then replaced with adipocyte media (Zen-Bio, Inc.) for 11 days. On day 14, cells were washed two times with 1 \times phosphate-buffered saline (Invitrogen) and fixed with 10% Formalin for 10 min. The cells were then stained with Oil Red O (Sigma-Aldrich, St. Louis, MO) for 1 h at room temperature, and digital images were captured using a phase contrast inverted Diaphot 300 microscope (Nikon, Tokyo, Japan) at a magnification of 10 \times .

Quantitation of Triglyceride in Differentiated Primary Human Preadipocytes. The intracellular triglyceride content within human preadipocytes differentiated for 14 days as described above with 0 to 10 μ M rosiglitazone, SPPAR γ M2, or nTZDpa was assayed with Adipored reagent using the protocol provided by the manufacturer (Lonza Bioscience, Basel, Switzerland).

Assessment of Gene Expression in Differentiated Primary Human Preadipocytes. RNA from primary human adipocytes differentiated for 14 days as described above with 10 μ M rosiglitazone, SPPAR γ M2, or nTZDpa was isolated using mRNA Catcher plates according to protocols from the manufacturer (Sequitur, Natick, MA). After reverse transcription of RNA using random hexamers, quantitative PCR of each target cDNA was performed with Taqman PCR reagent kits in the ABI Prism 7700 sequence detection system according to the protocols provided by the manufacturer (Applied Biosystems, Foster City, CA). The levels of mRNA were normalized to the amount of glyceraldehyde-3-phosphate dehydrogenase mRNA detected in each sample.

X-Ray Cocrytallography Studies of PPAR γ Ligands and the PPAR γ LBD. Purified PPAR γ LBD (residues Gln203 to Tyr477) (Berger et al., 2003) at 10 to 15 mg/ml was mixed with SPPAR γ M2 at a 1.1:1 M ratio of compound/protein on ice and allowed to stand at 4°C overnight. The solution was clarified, if necessary, by centrifugation before use. Crystals were grown by vapor diffusion at room temperature in 2- μ l "sitting" drops that contained equal volumes of the protein complex solution and a reservoir solution consisting of 100 mM Tris-HCl, pH 8.0, 0.65 to 0.90 M sodium citrate, and 1 mM tris(2-carboxyethyl) phosphine hydrochloride against 0.5 to 1.0 ml of reservoir solution in a Cryschem MVD-24 crystallization tray (Charles Supper, Natick, MA). Suitable crystals would appear in 1 to 3 weeks. Single crystals were transferred to 10 to 20 μ l of 100 mM Tris-HCl, pH 8.0, 1.44 M Na $_3$ citrate, and 1 mM tris(2-carboxyethyl) phosphine hydrochloride for 5 to 10 min at room temperature, and they were vitrified by plunging the nylon-loop-captured crystals directly into liquid nitrogen. Crystals were shipped overnight in a dry shipper at liquid nitrogen temperature to the Advanced Photon Source at Argonne National Laboratories (Argonne, IL). The dry shipper was refilled with liquid nitrogen, and single crystals were cryogenically transferred to a magnetic mount under a cold (-170°C) nitrogen gas stream generated by a CryoStream model 600 (Oxford

Cryosystems, Oxford, UK) for the duration of the diffraction experiment. X-ray diffraction data were collected at the ID-17 beamline of the Industrial Macromolecular Crystallography Association Collaborative Access Team as a series of 540 0.5° rotation images using an ADSC Quantum 210 2 \times 2 charge-coupled device area detector (Area Detection Systems Corporation, Poway, CA) mounted on a Crystal Logic goniometer (Crystal Logic, Los Angeles, CA). Exposure time was set to keep low-resolution reflection overloads at a minimum without significantly affecting the quality of the high-resolution data (1–3 s/exposure). Data were measured from a single crystal exhibiting C2 symmetry to a resolution of 2.0 Å. Measured intensities were reduced and scaled with DENZO and SCALEPACK from the HKL suite (Otwinowski and Minor, 1997) that yielded an average redundancy on measurements of approximately 5 and an R_{merge} of 0.042 (Table 1). The structure was solved by molecular replacement. SPPAR γ M2 was incorporated between rounds of model building using CHAIN (Sack, 1988) or XTALVIEW (McRee, 1999), and refinement was accomplished using CNX, version 2002 (Accelrys, San Diego, CA) (Brünger et al., 1987, 1998). A summary of the crystallographic data are found in Table 1. The quality of diffraction data is generally determined by the final resolution achieved (2.35 Å), the

TABLE 1
Crystallographic data summary for the cocrystal structure of SPPAR γ M2 with human PPAR γ LBD

Data Collection	Measurement
Space group	C2
Unit cell dimensions	a = 92.15 Å, b = 58.86 Å, c = 118.29 Å, β = 103.76°
No. of molecules per asymmetric unit	Two monomers
Resolution range (Å)	50.0–2.25 (2.35–2.25)
No. of observations	181,947
No. of unique reflections ^a	29,681 (3407)
I/ σ (I)	15.5 (2.51)
Completeness (%)	99.0 (93.7)
R_{sym} (%) ^b	0.042 (0.353)
Structure refinement	
Resolution range (Å)	40.34–2.25 (2.39–2.25)
$R_{\text{cryst}}/R_{\text{free}}$ (%) ^c	0.232/0.274 (0.324/0.383)
Protein atoms	3792
Water molecules	93
Ligand atoms	88
B-factor from Wilson plot (Å ²)	29.6
Average B-factor for all atoms (Å ²)	43.5
Cross-validated estimated coordinate error (Å) ^d	0.37
Root-mean-square deviation from expected geometry ^e	
Bond length (Å)	0.006
Bond angle (degrees)	0.9
Dihedral angle (degrees)	20.6
Improper angle (degrees)	0.66
Ramachandran statistics	
Residues in most favored regions (%)	91.9
Residues in additional allowed regions (%)	7.6
Residues in generously allowed region (%)	0.2
Residues in disallowed region (%)	0.2

^a A control set of 5% of these reflections, chosen randomly, were used to calculate an R_{free} to monitor the progress of refinement.

^b $R_{\text{sym}} = \sum_j | \langle I_i \rangle - I_{ij} | / \sum_j \langle I_i \rangle$, where $\langle I_i \rangle$ is the mean intensity of the i th reflection, and I_{ij} is the symmetry related j th measurement of the i th reflection.

^c $R_{\text{cryst}} = \sum | | F_{\text{obs}} | - | F_{\text{calc}} | | / \sum | F_{\text{obs}} |$, where $| F_{\text{obs}} |$ and $| F_{\text{calc}} |$ are the calculated and observed structure factor amplitudes, respectively, for the 95% of reflections used in refinement. R_{free} is calculated in the same manner using only the control set of reflections.

^d Luzzati48 method was used along with the control set of reflections used to calculate R_{free} .

^e Engh and Huber49 stereochemical parameters were used in the refinement.

number of unique reflections collected (29,681, or 99.0% of all data to 2.35 Å) compared with the number of nonhydrogen atoms in the model (3973, or 7.5 reflections/atom), and how well the individual diffraction measurements combine with each other ($R_{\text{sym}} < 10\%$ overall). The quality of the atomic model is best judged visually by how well it fits the electron density derived from the experimental data. However, resolution (< 2.5 Å) will indicate the expected level of detail to be seen, $R_{\text{cryst}} (< 25)/R_{\text{free}} (< 30)$ will provide estimates of how well diffraction data calculated from the model will compare with the experimentally collected data. Plotting the two main chain angles (ϕ and ψ) for each residue on a Ramachandran plot ($> 90\%$ in most favored regions and 0% in disallowed regions for nonglycine residues) and determining the root mean square deviations of bond lengths, bond angles, etc., provides additional support for the accuracy of the atomic model. The coordinates may be found in the Protein Data Bank under ID code 2P4Y.

Results

Identification of Novel SPPAR γ M_s. To identify novel SPPAR γ M_s, a series of indole-containing small molecules were chemically synthesized (Acton et al., 2005; Dropinski et al., 2005; Liu et al., 2005) and characterized by two in vitro pharmacological assays. First, we determined which of the compounds were PPAR γ ligands by performing SPA-based competition binding assays as described previously (Berger et al., 2003). Subsequently, we carried out PPAR γ cell-based transcriptional activity assays as described previously (Berger et al., 1999) to assess the functional activities of the ligands. Through these efforts, we were able to identify a series of novel indole-containing SPPAR γ M_s that demonstrate $< 40\%$ of the maximal PPAR γ transcriptional activity of rosiglitazone (Table 2). An example of such a compound is SPPAR γ M2, which was able to completely displace the radioligand [$^3\text{H}_2$]nTZD3 from PPAR γ , with greater potency than rosiglitazone in competition binding assays (Fig. 1A). SPPAR γ M2 also activated the receptor with greater potency than rosiglitazone but only to a maximal level that was $\sim 20\%$ of that attained with the full agonist (Fig. 1B). The same binding and transcriptional activity assays were used to identify and characterize a cohort of structurally diverse PPAR γ full agonists that possess $100 \pm 30\%$ of the maximal PPAR γ transcriptional activity of rosiglitazone (Table 2).

SPPAR γ M_s Induced Diminished Adipogenic Differentiation of Human Preadipocytes Compared with PPAR γ Full Agonists. The essential role of PPAR γ in adipocyte differentiation and the robust effects of PPAR γ full agonists on adipogenesis are well established (Berger et al., 2005). We have demonstrated that the SPPAR γ M nTZDpa had a diminished ability to induce adipogenic differentiation of mouse 3T3-L1 preadipocytes in comparison with PPAR γ full agonists such as rosiglitazone (Berger et al., 2003); similar studies with SPPAR γ M2 provided comparable results (data not shown). To extend this observation by assessing the human adipogenic potential of SPPAR γ M_s, we first examined the effects of SPPAR γ M2, nTZDpa, and rosiglitazone on lipid accumulation in human subcutaneous preadipocytes. At day 14 of the differentiation regimen, the lipid content within the cells was first assessed by microscopic examination of cells stained with Oil Red O and then by a quantitative fluorescent lipid accumulation assay using Adipored reagent as described under *Materials and Methods*. Micrographs presented in Fig. 2A demonstrate that incubation of the preadi-

pocytes with SPPAR γ M2 resulted in the generation of fewer lipid-containing adipocytes than rosiglitazone. Consistent with these results, data from the Adipored assay indicated that although both the SPPAR γ M_s and rosiglitazone promoted lipid accumulation in a dose-responsive manner, maximum lipid accretion by cells incubated with the SPPAR γ M_s was greatly diminished compared with those treated with the full agonist (Fig. 2B).

The adipogenic activity of PPAR γ activators are apparently mediated by their ability to alter the expression of gene constellations that regulate various elements of the adipocytic phenotype. A number of genes that are regulated by PPAR γ , including the direct, PPAR-response element-containing targets FABP4, PEPCK, and ADFP, have been shown to serve as markers of adipocyte differentiation (Hunt et al., 1986; Jiang and Serrero, 1992; Tontonoz et al., 1995). Therefore, we isolated RNA from cells that had undergone 14 days of adipogenic differentiation, and we compared the regulatory effects of SPPAR γ M_s and rosiglitazone on the expression of these three genes. As demonstrated in Fig. 2C, SPPAR γ M2 and nTZDpa displayed a diminished ability to induce FABP4, PEPCK, and ADFP mRNA expression compared with rosiglitazone. Taken together, our data indicate that SPPAR γ M_s are less effective than a prototypical PPAR γ full agonist in promoting adipogenesis of human preadipocytes.

SPPAR γ M2 Did Not Interact with the PPAR γ LBD in the Vicinity of Tyr473. The hPPAR γ -LBD/SPPAR γ M2 complex crystallized with a monoclinic habit that contains two monomers in the asymmetric unit (a side-by-side view of the two monomers is depicted in Fig. 3). Monomer A assumed an “activated” conformation with the displaced helix 12 of a symmetry-related monomer occupying the coactivator peptide binding site, stabilizing the position of the local helix 12 so that the side chain of residue Tyr473 was pointing into the ligand binding pocket. It should be noted that the binding of the coactivator peptide analog (sequence H466-P-L-L-Q-E-I472) binds to monomer A in the same orientation seen in the ternary complex of hPPAR γ -LBD/rosiglitazone/SRC-1 peptide (Nolte et al., 1998), but the “charge clamp” residues Lys301 and Glu471 do not make direct hydrogen bonds to the backbone atoms of the bound helix. Monomer B, in contrast, assumed an “unactivated” conformation with the connected helix 12 displaced so that Tyr473 is unable to enter the ligand binding pocket. Furthermore, there was very little strong and continuous electron density for the connecting loop between helices 11 and 12 to allow for the unambiguous placement of residues 457 to 465. Other regions of considerable flexibility common to both monomers include the elbow between helix 2 and β strand 1 (residues 238–244) and the insert region between β strand 1 and helix 3 (residues 255–278). Model coordinates are omitted for these regions. In spite of this, SPPAR γ M2 bound to both monomers in the same configuration, with the carboxylic acid hydrogen bonded to the main-chain nitrogen atom of Ser342 (Fig. 4). In monomer A only, there was additional electron density between the bound SPPAR γ M2 and the residues that typically interact with the acid functionalities of full agonists His323, His449, and Tyr473. The shape of this density was consistent with tris(hydroxymethyl)-aminomethane, the buffer molecule that is present at nearly 100 mM, and has been modeled as such. How-

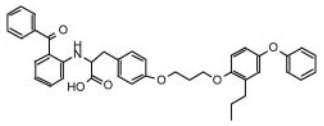
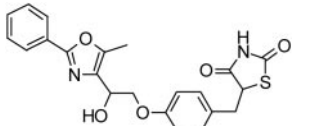
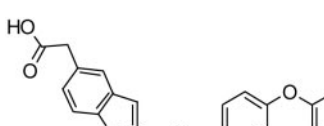
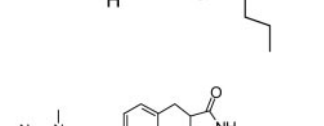
TABLE 2
 Properties of PPAR γ ligands

Ligand	Structure	PPAR γ WT K_i	PPAR γ Y473A K_i	PPAR γ WT EC $_{50}$	PPAR γ Y473A EC $_{50}$	PPAR γ WT
		μM				% ^a
SPPAR γ M1		0.003	0.003	0.005	0.003	18
SPPAR γ M2		0.001	0.001	0.003	0.003	18
SPPAR γ M3		0.005	0.007	0.002	0.001	13
SPPAR γ M4		0.053	0.051	0.037	0.047	13
SPPAR γ M5		0.040	0.047	0.053	0.067	20
SPPAR γ M6		0.027	0.030	0.023	0.016	24

TABLE 2 (Continued)

Ligand	Structure	PPAR γ WT K_i	PPAR γ Y473A K_i	PPAR γ WT EC $_{50}$	PPAR γ Y473A EC $_{50}$	PPAR γ WT
		μM				% ^a
SPPAR γ M7		0.049	0.076	0.028	0.036	32
SPPAR γ M8		0.024	0.022	0.002	0.002	38
nTZDpa		0.145	0.270	0.140	0.142	33
Full1		0.016	0.077	0.015	0.115	70
Full2		0.675	6.667	0.028	>3.000	70
Full3		1.252	4.803	0.056	0.584	74

TABLE 2 (Continued)

Ligand	Structure	PPAR γ WT K_i	PPAR γ Y473A K_i	PPAR γ		PPAR γ WT EC $_{50}$	PPAR γ Y473A EC $_{50}$	PPAR γ WT EC $_{50}$	PPAR γ WT EC $_{50}$
				μ M	% ^a				
Full4		0.446	4.912	0.015	>3.000				99
Full5		0.066	5.578	0.003	1.630				105
TZDfa		0.272	>15	0.003	0.666				130
COOH		1.054	>15	0.343	>3.000				70
Rosiglitazone		0.992	>15	0.019	>3.000				100

^a Percentage of maximal activity in cell-based transcriptional activity assay vs. rosiglitazone.

ever, this density may instead indicate the presence of a low (<5%) occupancy conformation of the bound SPPAR γ M2 that may have bound as a full agonist with the compound's carboxylic acid interacting directly with the phenolic hydroxyl of Tyr473.

Effect of the Y473A Mutation on the Functional Activity of PPAR γ Ligands. We and others have provided X-ray cocrystallography and molecular modeling data supporting the proposition that PPAR γ full agonists interact directly with the Tyr473 residue in helix 12 of the LBD of the receptor, whereas SPPAR γ Ms do not (Oberfield et al., 1999; Burgermeister et al., 2006). To directly determine the functional importance of this differential receptor-ligand interaction, we used recombinant mutagenesis techniques to change the Tyr473 residue of PPAR γ to an alanine. The activities of SPPAR γ M2 and rosiglitazone were then examined in transcriptional activity assays performed as described previously (Berger et al., 1999) in COS-1 cells transiently transfected with a GAL4-responsive reporter construct and a chimeric receptor composed of the GAL4 DNA-binding domain and either the hPPAR γ WT or hPPAR γ Y473A LBD. As seen in Fig. 5A, the activity of rosiglitazone was nearly completely abrogated with hPPAR γ Y473A compared with hPPAR γ WT. In contrast, only a negligible alteration in SPPAR γ M2 potency was seen between the mutant and wild-type recep-

tors. Furthermore, when the activities of numerous structurally diverse PPAR γ full agonist and SPPAR γ M collections were determined in similar transactivation assays with hPPAR γ WT and hPPAR γ Y473A, it was clearly demonstrated that there were marked reductions in activation maxima and potency for full agonists but not with SPPAR γ Ms (Table 2; Fig. 5B). To directly probe the significance of the carboxylic acid on SPPAR γ M activity, the alkynyl-substituted SPPAR γ M4, which is completely devoid of the acidic moieties present in on all other ligands, was synthesized. SPPAR γ M4 exhibited comparable binding and functional activity in hPPAR γ WT and hPPAR γ Y473A assays. In cocrystallization studies with hPPAR γ -LBD, SPPAR γ M4 was found in the same position and orientation observed for SPPAR γ M2 (our unpublished data). Rather than interact with the Ser342 NH like the carboxylate, the alkynyl substituent extended directly toward bulk solvent adjacent to the C α of Gly284. The ~15-fold decrease in potency observed when comparing the carboxylate SPPAR γ M1 with its alkynyl analog SPPAR γ M4 was commensurate with what might be expected for loss of a neutral-neutral hydrogen bond rather than for a charge-reinforced hydrogen bond, perhaps as a consequence of exposure to bulk solvent (Davis and Teague, 1999). These data further support the novel binding model (Schupp et al., 2005; Burgermeister et al.,

2006) discussed for SPPAR γ M2 and the lack of direct interactions with Tyr473.

Development of Novel hPPAR γ WT and hPPAR γ -Y473A and SPA Binding Assays. Having identified a negative effect of the Y473A mutation on the functional activities of PPAR γ full agonists, it was necessary to confirm whether these changes were due to a reduction in the intrinsic binding affinities of these ligands or whether defective functional activation occurred despite normal binding potency. Thus, we developed ligand binding assays that could be used to compare the potencies of full agonists and SPPAR γ M2s with hPPAR γ WT and hPPAR γ Y473A. We could not use our previously reported radioligand [3 H]nTZD3 (Berger et al., 2003) for such studies, because it is a full agonist that demonstrated greatly diminished potency with hPPAR γ Y473A in transcriptional activity assays similar to those described above (data not shown). Thus, SPPAR γ M1 was selected as a candidate radioligand with which to develop parallel binding assays, because its functional activity was unaffected by the Y473A mutation (Table 1).

Using [3 H]SPPAR γ M1 as the radioligand at concentrations from 0 to 30 nM in the presence or absence of 50 μ M excess

cold SPPAR γ M1, saturation binding assays were performed with recombinant hPPAR γ WT LBD or hPPAR γ Y473A LBD, as described under *Materials and Methods*. Nonlinear regression analyses of data from these studies indicated that the Y473A mutation did not have a significant effect on SPPAR γ M1 binding, because its K_d value was determined to be 1.83 and 1.60 nM for hPPAR γ WT (Fig. 6A) and hPPAR γ Y473A (Fig. 6B), respectively. Therefore, [3 H]SPPAR γ M1 proved to be a suitable radioligand for subsequent competition binding assays with

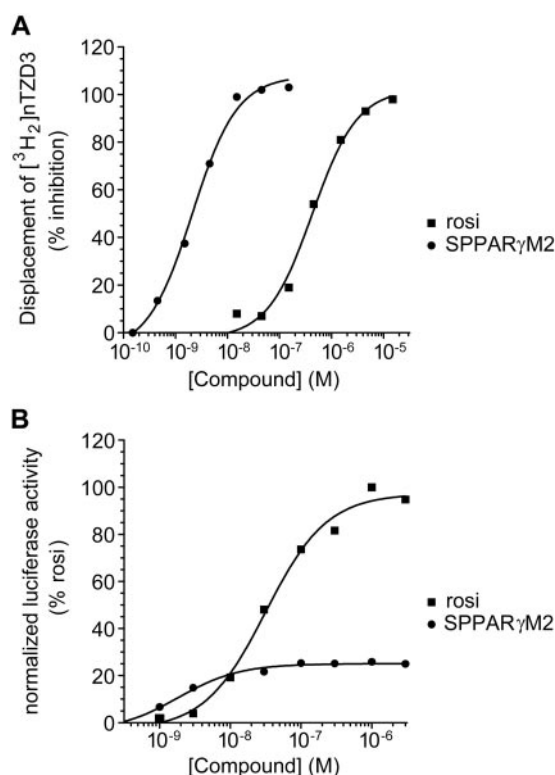


Fig. 1. SPPAR γ M2 is a potent PPAR γ ligand and partial agonist. A, binding of SPPAR γ M2 and rosiglitazone to PPAR γ . Competition binding curves were generated by incubation of 5 nM [3 H]nTZD3 with GST-hPPAR γ . The displacement of radioligand after incubation in the presence of the indicated concentrations of SPPAR γ M2 or rosiglitazone for 16 h is plotted. Similar results were obtained in at least two independent experiments performed in duplicate. B, activation of hPPAR γ by SPPAR γ M2 or rosiglitazone. COS-1 cells were transiently cotransfected with pSG5-hPPAR γ /GAL4, pUAS(5X)-tk-luciferase and pCMV-lacZ, and then they were incubated with the indicated concentrations of rosiglitazone, SPPAR γ M2, or rosiglitazone for 48 h. Cell lysates were produced, and luciferase and β -galactosidase activity in cell extracts was determined. The means of triplicate samples from a representative experiment are plotted. Similar results were obtained in at least two independent experiments.

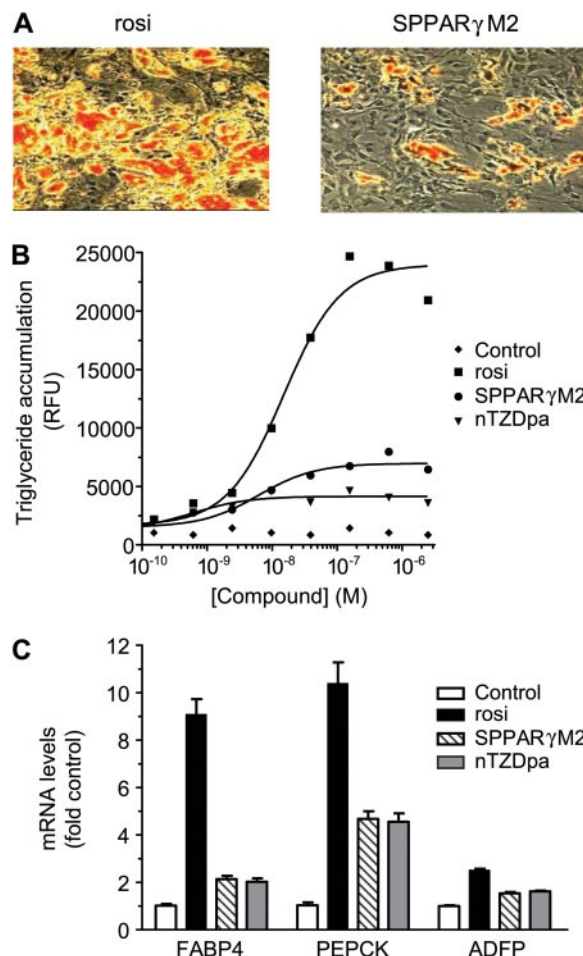


Fig. 2. SPPAR γ M2s display diminished adipogenic action on human preadipocytes in comparison with a PPAR γ full agonist. A, differentiation of preadipocytes into lipid-filled adipocytes. Primary human preadipocytes derived were differentiated by adding 10 μ M rosiglitazone or SPPAR γ M2 for 5 days. The differentiation media were then replaced with adipocyte media for 11 days. On day 14, cells were washed, fixed, and stained with Oil Red O, and then phase contrast micrographs were taken at 10 \times magnification. B, quantitation of triglyceride in differentiated primary human preadipocytes. The triglyceride content of human preadipocytes differentiated for 14 days as described above with 0 to 10 μ M rosiglitazone, SPPAR γ M2, or nTZDpa was assayed with Adipored reagent as described under *Materials and Methods*. The means of triplicate samples from a representative experiment are plotted. Similar results were obtained in at least two independent experiments. C, determination of adipocyte marker gene expression in differentiated primary human adipocytes. RNA from primary human adipocytes differentiated for 14 days as described above with 10 μ M rosiglitazone, SPPAR γ M2, or nTZDpa was isolated and reverse transcribed. Quantitative PCR of FABP4, PEPCK, and ADFP cDNA was performed, and the level of each mRNA was normalized to the amount of glyceraldehyde-3-phosphate dehydrogenase mRNA detected in each sample. The figure plots the mean \pm S.E.M. of triplicate samples of a representative experiment. Similar results were obtained in at least two independent experiments.

which to compare the intrinsic potencies of PPAR γ full agonists and SPPAR γ M γ s.

Binding Potencies of PPAR γ Full Agonists but Not SPPAR γ M γ s Were Diminished with the hPPAR γ Y473A Mutant. In initial experiments, we compared the binding of rosiglitazone and SPPAR γ M2 to hPPAR γ WT and hPPAR γ -Y473A in SPA assays using [3 H]SPPAR γ M1. The affinity of the full agonist but not the SPPAR γ M was greatly reduced

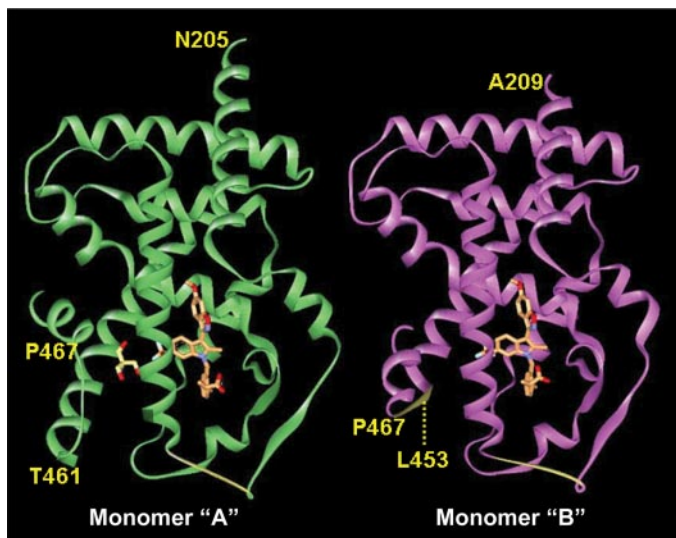


Fig. 3. The hPPAR γ LBD crystallizes as an asymmetric unit containing activated and unactivated forms of the receptor monomer. The two monomers of the asymmetric unit are depicted side by side to highlight structural differences between the activated form on the left and the unactivated on the right. SPPAR γ M2 and tris(hydroxymethyl)-aminomethane are depicted with orange and yellow carbons, respectively. Regions of missing density are depicted as light yellow strands. The crystals were generated and analyzed as described under *Materials and Methods*.

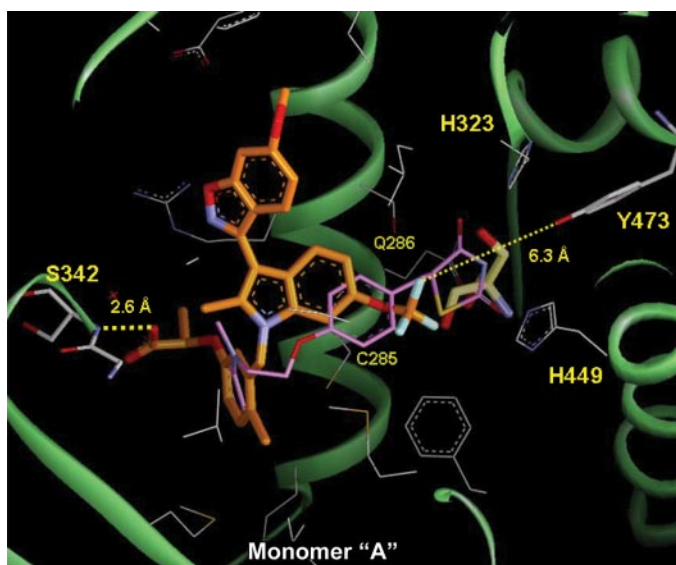


Fig. 4. SPPAR γ M2 interacts with different residues within the hPPAR γ LBD than rosiglitazone. View of SPPAR γ M2 (orange) and “tris” (yellow) as cocrystallized with hPPAR γ and residues that fall within 5 Å of either. Rosiglitazone (purple) as cocrystallized with hPPAR γ (Protein Data Bank under ID code 2PRG) references the binding orientation for the typical agonist.

with the mutant receptor in comparison with the wild-type receptor (Fig. 7A). Subsequently, the binding potencies of the same diverse collection of SPPAR γ M γ s and PPAR γ full agonists studied in the aforementioned cell-based transcriptional activity assays were determined in the competition binding assays. Data from these studies revealed that PPAR γ full agonists consistently displayed a marked reduction in binding affinity to hPPAR γ Y473A in comparison with hPPAR γ WT (Fig. 7B). In contrast, the binding characteristics of the SPPAR γ M γ s were not notably affected by the Y473A mutation. Such results largely paralleled those obtained previously in the transcriptional activity assays described above. In fact, the shifts in potencies of the tested ligands in the two assays were highly correlated: $r^2 = 0.86$, $p < 0.0001$ (Fig. 8).

Discussion

PPAR γ agonists, including the currently marketed TZDs pioglitazone and rosiglitazone, have proven efficacious in the

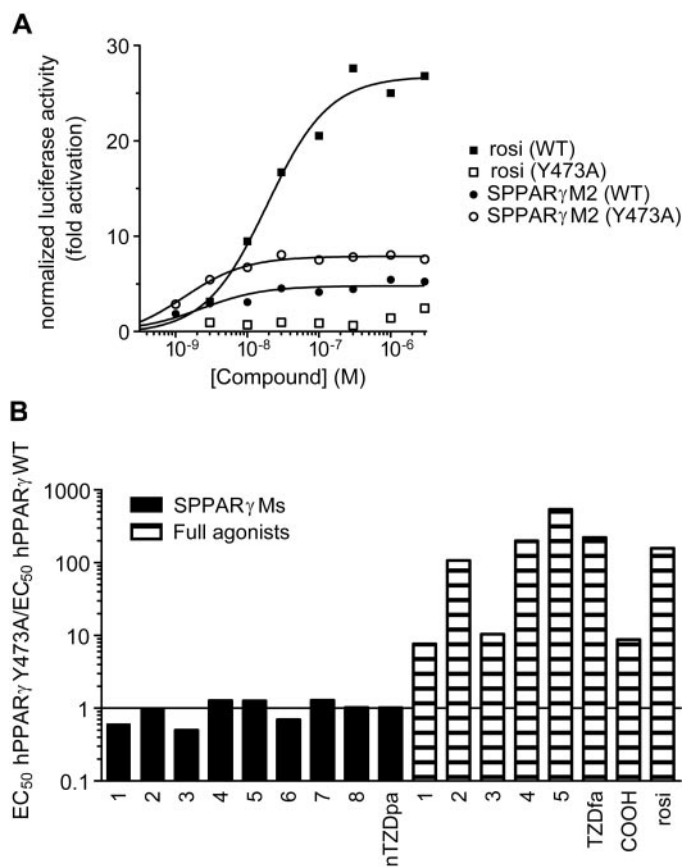


Fig. 5. Transcriptional activities of PPAR γ full agonists but not SPPAR γ M γ s are diminished with PPAR γ Y473A versus PPAR γ WT. A, activation of PPAR γ WT and PPAR γ Y473A by rosiglitazone or SPPAR γ M2. COS-1 cells were transiently cotransfected with pcDNA3-hPPAR γ WT/GAL4 or pcDNA3-hPPAR γ Y473A/GAL4 and both pUAS(5X)-tk-luciferase and pCMV-*lacz*, and then they were incubated with the indicated concentrations of rosiglitazone or SPPAR γ M2 for 48 h. Cell lysates were produced, luciferase, and β -galactosidase activities in cell extracts were determined as. The figure plots the mean \pm S.E.M. of triplicate samples of a representative experiment. Similar results were obtained in at least two independent experiments. B, ratio of potencies of SPPAR γ M γ s and PPAR γ full agonists in the hPPAR γ WT and hPPAR γ Y473A transcriptional activity assays. Assays were performed as described above, and EC $_{50}$ values were determined by four-parameter fit analysis. The figure plots the EC $_{50}$ hPPAR γ Y473A/EC $_{50}$ hPPAR γ WT ratios for the PPAR γ ligands.

treatment of T2DM patients. However, despite the significant antidiabetic activity of such compounds, they have been used in a limited manner because of several untoward effects associated with their use. These include plasma volume expansion and edema, which can lead to or exacerbate congestive heart failure, as well as weight gain resulting from increased adiposity and plasma volume. To extend PPAR γ -targeted diabetes therapy to a broader patient population, considerable efforts have recently focused on the identification of novel efficacious PPAR γ ligands with improved tolerability. Such endeavors have been motivated by the success of previous drug researchers in identifying selective modulators of steroid nuclear receptors that demonstrated cell-, tissue-, and gene-specific activities (Miller, 2002). For example, selective estrogen receptor modulators were found to retain beneficial effects in the treatment of osteoporosis while inducing diminished

adverse effects. Thus, we and others have proceeded to generate and characterize SPPAR γ M_s that might serve as an improved second generation of insulin-sensitizing agents for the amelioration of T2DM and other metabolic disorders.

Here, we present examples of novel indole-containing SPPAR γ M_s that are structurally distinct from such ligands described previously by ourselves and others (Berger et al., 2003; Minoura et al., 2004; Acton et al., 2005; Dropinski et al., 2005; Schupp et al., 2005; Burgermeister et al., 2006). These SPPAR γ M_s were identified by their ability to bind the PPAR γ with high affinity and to serve as potent partial agonists of the receptor in cell-based transcriptional activity assays. Additional studies performed on an exemplary member of this cohort, SPPAR γ M₂, revealed that in comparison with PPAR γ full agonists, this ligand (like nTZDpa) possessed reduced adipogenic activity and an attenuated regulatory effect on the PPAR γ target genes FABP4, PEPCK, and ADFP in human adipocytes. These

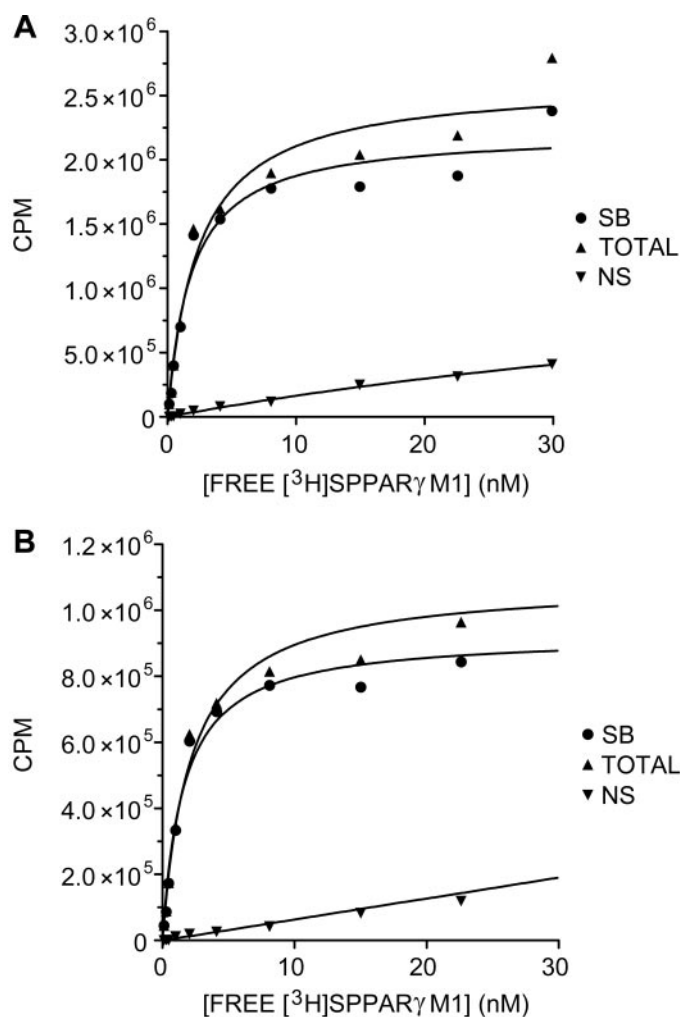


Fig. 6. Radiolabeled SPPAR γ M₁ is a potent ligand of hPPAR γ WT and hPPAR γ Y473A. A, nonlinear regression analysis of data from hPPAR γ WT saturating binding studies performed using GST-hPPAR γ WT LBD, anti-GST antibody, and radioligand [³H]SPPAR γ M₁ at 0 to 30 nM \pm 50 mM cold SPPAR γ M₁. B, nonlinear regression analysis of data from hPPAR γ Y473A saturating binding studies performed using GST-hPPAR γ Y473A LBD, anti-GST antibody, and radioligand [³H]SPPAR γ M₁ at 0 to 30 nM \pm 50 μ M cold SPPAR γ M₁. Similar results were obtained in two independent experiments performed in duplicate.

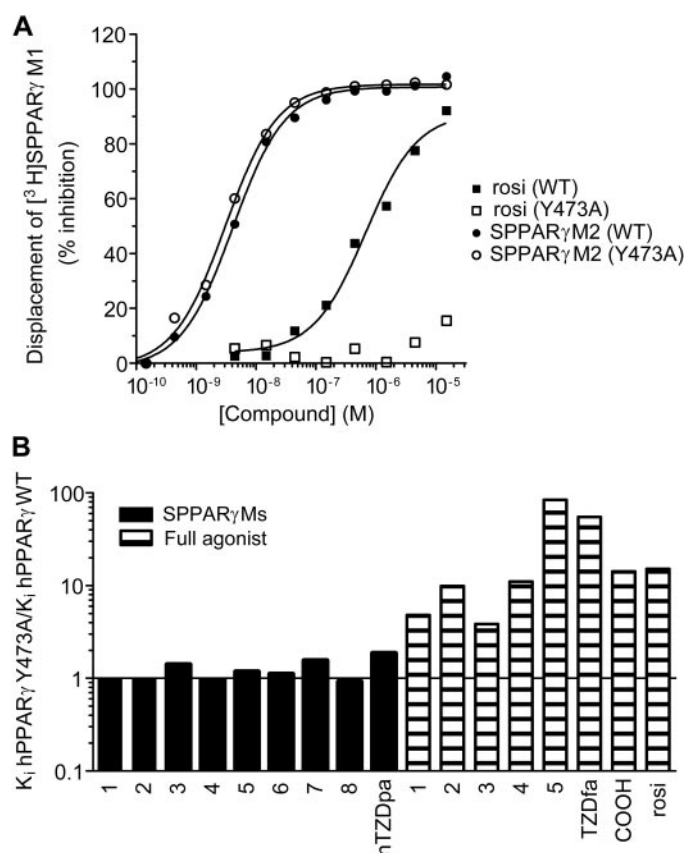


Fig. 7. Binding potencies of PPAR γ agonists but not SPPAR γ M_s are diminished with hPPAR γ Y473A versus hPPAR γ WT. A, binding of SPPAR γ M₂ and rosiglitazone to PPAR γ WT and hPPAR γ Y473A. Competition curves generated by incubation of 2.5 nM [³H]SPPAR γ M₁ with GST-hPPAR γ WT LBD or GST-hPPAR γ Y473A LBD. The displacement of radioligand after incubation in the presence of the indicated concentration of SPPAR γ M₂ or rosiglitazone is plotted. Similar results were obtained in at least two independent experiments performed in duplicate. B, ratio of potencies of SPPAR γ M_s and PPAR γ full agonists in the hPPAR γ WT and hPPAR γ Y473A transcriptional activity assays. Assays were performed as described above, and K_1 values were determined by four-parameter fit analysis. The figure plots the K_1 hPPAR γ Y473A/ K_1 hPPAR γ WT ratios for the PPAR γ ligands.

findings extend and concur with those obtained previously with SPPAR γ M_s in mouse 3T3-L1 cells and adipose tissue (Oberfield et al., 1999; Berger et al., 2003; Schupp et al., 2005).

X-ray studies of the PPAR γ LBD cocrystallized with the PPAR γ full agonist rosiglitazone support the proposition that the negatively charged nitrogen of the TZD head group forms a hydrogen bond with the helix 12 Tyr473 side-chain hydroxyl head group (Nolte et al., 1998). Additional hydrogen bond interactions are thought to exist between the ligand and the His323, His449, and Lys367 residues. These interactions govern the conformation of the TZD head group and the amino acids of the ligand binding domain. In subsequent X-ray crystallography studies, the carboxylic acid moiety of the tyrosine-based PPAR γ full agonist GI262570 and an α -aryloxyphenylacetic-derived PPAR γ/α agonist were also shown to reside within hydrogen binding distance of the Tyr473 moiety of the PPAR γ LBD (Gampe et al., 2000; Shi et al., 2005). In contrast, crystal structures of the PPAR γ LBD with the structurally distinct SPPAR γ M_s GW0072 (Oberfield et al., 1999), PA-082 (Burgermeister et al., 2006), and SPPAR γ M2 (data above) revealed that these ligands were bound in the entry-end of the ligand binding pocket at a distance from helix 12 that preclude direct contact with Tyr473.

As depicted in Fig. 4 for monomer A, the phenolic O of Tyr473 was more than 6 Å removed from its closest approach to SPPAR γ M2 at the trifluoromethyl tail. Nor is Tyr473 properly positioned to hydrogen bond with tris(hydroxymethyl)-aminomethane, which instead apparently hydrogen bonded to the Gln286, His323, and His449 side chains. As a result of the repositioning of helix 12, Tyr473 was situated outside of the binding cavity in monomer B. Other than this difference, the rest of the residues proximate to the partial agonist were the same in either monomer and similarly situated to create the hydrophobic interior to the binding cavity. A unique consequence of the

meta-substitution pattern is that the lactate was unable to achieve a conformation that would allow it, like its *ortho*-substituted analog Full1, to act as a potent full agonist presumably via hydrogen bonding to Tyr473 (Acton et al., 2005). Rather, this structural constraint forced the lactate to hydrogen bond with the main-chain NH of Ser342. This interaction was similar to that observed crystallographically for a 2-benzoylaminobenzoic acid analog complexed with hPPAR γ (Ostberg et al., 2004), and it was quite distinct from that seen between agonists such as rosiglitazone and Tyr473 as in Fig. 4.

On the basis of the above-mentioned observations, we first assessed the role of Tyr473 in determining the functional activities of structurally diverse PPAR γ full agonists and SPPAR γ M_s in cell-based transcriptional activity assays using wild-type hPPAR γ and a mutant receptor in which the tyrosine residue 473 in helix 12 was mutated to an alanine. We found that the clinically available PPAR γ full-agonist rosiglitazone underwent a large diminution in activity with hPPAR γ Y473A compared with hPPAR γ WT. Moreover, we also provide evidence indicating that Tyr473 was also required for the activity of a variety of structurally distinct TZD and non-TZD full agonists. In striking contrast to these results, the Tyr473A mutation did not influence the functional activity of SPPAR γ M2, nTZDpa, or the remainder of the structurally diverse SPPAR γ M_s that were tested.

To clarify whether the observed decreases in functional activity of PPAR γ full agonists were due to decreases in their intrinsic binding potencies or reduced ability of such ligands to induce a productive receptor conformation after binding in the LBD, we developed a novel SPA-based competition binding assay for hPPAR γ WT and hPPAR γ Y473A using [³H]SPPAR γ M1 as the radioligand. We found that [³H]-SPPAR γ M1 was well suited for this purpose, because, in concordance with cell-based transactivation studies showing that its functional activity was not significantly affected by the Y473A mutation, nonlinear regression analyses of ligand binding studies revealed that the Y473A mutation had a negligible influence on the affinity of [³H]SPPAR γ M1 for PPAR γ .

When the binding activities of the PPAR γ full agonist rosiglitazone and SPPAR γ M2 were examined in radioligand displacement assays using [³H]SPPAR γ M1, we found that the potency of the full agonist was decreased more than 10-fold with hPPAR γ Y473A in comparison with hPPAR γ WT, whereas the affinity of SPPAR γ M2 was undiminished by the Y473A mutation. In subsequent binding assays performed with our full array of PPAR γ full agonists and SPPAR γ M_s, all of the former ligands underwent notable decreases in potency with the mutant receptor that correlated well with the similar large reductions in potencies observed with PPAR γ Y473A in the transcriptional activity studies. Thus, Tyr473 was clearly required for both receptor binding and subsequent activation by PPAR γ full agonists; in contrast, the SPPAR γ M_s demonstrated similar potencies in binding assays performed with hPPAR γ WT and hPPAR γ Y473A. Such results support the proposition that the SPPAR γ M_s retained their functional activities with hPPAR γ Y473A because their intrinsic binding activities were largely unchanged with the mutant receptor.

Taken together, our results provide robust biochemical support for the X-ray crystallography data from our studies

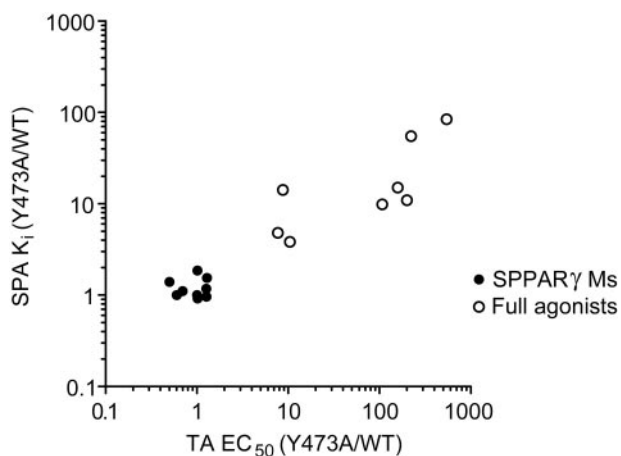


Fig. 8. Diminished functional potencies of PPAR γ full agonists with hPPAR γ Y473A versus hPPAR γ WT correlate with their diminished binding potencies with hPPAR γ Y473A versus hPPAR γ WT. The EC₅₀ hPPAR γ Y473A/EC₅₀ hPPAR γ WT and the K_i hPPAR γ Y473A/K_i hPPAR γ WT ratios of the PPAR γ ligands presented in Table 2 were plotted against each other on log₁₀ scale x- and y-axes.

as well as those of others indicating that PPAR γ full agonists but not SPPAR γ Ms interact directly with the Tyr473 residue located in the activation function-2 helix of the PPAR γ LBD (Oberfield et al., 1999; Burgermeister et al., 2006). Although Tyr473 is not a component of the charge clamp that contacts backbone atoms of LXXLL helices within transcriptional coactivators, it is in proximity to Glu471, one of the two major residues implicated in this PPAR γ -coactivator interaction (Nolte et al., 1998; Sheu et al., 2005). We have previously shown by NMR spectroscopy studies that PPAR γ full agonists induce a more stable conformation of the PPAR γ LBD, including the helix 12, than SPPAR γ Ms (Berger et al., 2003). Thus, the differing abilities of PPAR γ full agonists and SPPAR γ Ms to interact with Tyr473 and directly stabilize the aforementioned charge clamp seem to result, at least in part, in the differential receptor-coactivator interactions that have been observed with these two classes of ligands, thereby serving as a physical basis for their distinct gene transcription and resulting pharmacological effects. In support of this proposition, it has been demonstrated that compared with PPAR γ full agonists such as rosiglitazone or pioglitazone, the structurally distinct SPPAR γ Ms telmisartan, irbesartan, PA-082, and FK-614 induce diminished interaction of PPAR γ with transcriptional coactivators, including transcriptional intermediary factor 2, steroid receptor coactivator 1, and CREB-binding protein, that was associated with attenuated adipocyte gene regulation by the latter ligands (Schupp et al., 2005; Burgermeister et al., 2006; Fujimura et al., 2006). In addition, when two of these SPPAR γ Ms, telmisartan and FK614, were studied in rodent models of T2DM, they displayed comparable insulin-sensitizing activity to PPAR γ full agonists with reduced mechanism-based adverse effects, including hemodilution, cardiomegaly, and body weight gain (Minoura et al., 2004; Schupp et al., 2005).

In summary, we have presented data demonstrating that a novel selective PPAR γ modulator, SPPAR γ M2, is a potent PPAR γ ligand that displays diminished maximal activity compared with the PPAR γ full agonist rosiglitazone in cell-based assays of transcriptional and adipogenic activity. In additional studies using the wild-type and mutant receptors, hPPAR γ WT and hPPAR γ Y473A, respectively, to characterize the binding and functional activities of structurally distinct PPAR γ full agonists and SPPAR γ Ms, we demonstrated that the LBD helix 12 residue Tyr473 plays a critical role in the interaction of the former but not the latter ligands with the receptor. Such results provide a physical basis for the novel biological activities of SPPAR γ Ms. Finally, it is worth noting that based on our results, hPPAR γ Y473A might prove useful as the basis for a high-throughput assay that would be biased toward the identification of additional, structurally unique SPPAR γ Ms. Thus, by advancing our understanding of PPAR γ molecular pharmacology and structural biology, we hold the potential to further enrich a population of ligands that should prove useful in further probing PPAR γ biology and that may provide novel PPAR γ -targeted therapeutic agents of superior efficacy and tolerability than are currently available for the treatment of T2DM patients.

Acknowledgments

We thank the Merck Research Laboratories medicinal chemists for providing the Merck ligands used in this study. We are grateful for the technical assistance of Neelam Sharma.

References

- Acton JJ 3rd, Black RM, Jones AB, Moller DE, Colwell L, Doebber TW, Macnaul KL, Berger J, and Wood HB (2005) Benzoyl 2-methyl indoles as selective PPAR γ modulators. *Bioorg Med Chem Lett* **15**:357–362.
- Berger J, Leibowitz MD, Doebber TW, Elbrecht A, Zhang B, Zhou G, Biswas C, Cullinan CA, Hayes NS, Li Y, et al. (1999) Novel PPAR γ and PPAR δ ligands produce distinct biological effects. *J Biol Chem* **274**:6718–6725.
- Berger J and Moller DE (2002) The mechanism of action of PPARs. *Annu Rev Med* **53**:409–435.
- Berger JP, Akiyama TE, and Meinke PT (2005) PPARs: therapeutic targets for metabolic disease. *Trends Pharmacol Sci* **26**:244–251.
- Berger JP, Petro AE, Macnaul KL, Kelly LJ, Zhang BB, Richards K, Elbrecht A, Johnson BA, Zhou G, Doebber TW, et al. (2003) Distinct properties and advantages of a novel peroxisome proliferator-activated receptor [gamma] selective modulator. *Mol Endocrinol* **17**:662–676.
- Brünger AT, Adams PD, Clore GM, DeLano WL, Gros P, Grosse-Kunstleve RW, Jiang JS, Kuszewski J, Nilges M, Pannu NS, et al. (1998) Crystallography & NMR system: a new software suite for macromolecular structure determination. *Acta Crystallogr D Biol Crystallogr* **54**:905–921.
- Brünger AT, Kuriyan J, and Karplus M (1987) Crystallographic R-factor refinement by molecular dynamics. *Science* **235**:458–460.
- Burgermeister E, Schnoebelen A, Flament A, Benz J, Stihle M, Gsell B, Rufer A, Ruf A, Kuhn B, Marki HP, et al. (2006) A novel partial agonist of peroxisome proliferator-activated receptor-gamma (PPAR γ) recruits PPAR γ -coactivator-1 α , prevents triglyceride accumulation, and potentiates insulin signaling in vitro. *Mol Endocrinol* **20**:809–830.
- Davis AM and Teague SJ (1999) Hydrogen bonding, hydrophobic interactions and failure of the rigid receptor hypothesis. *Angew Chem Int Ed Engl* **30**:736–749.
- Dropinski JF, Akiyama T, Einstein M, Habulihaz B, Doebber T, Berger JP, Meinke PT, and Shi GQ (2005) Synthesis and biological activities of novel aryl indole-2-carboxylic acid analogs as PPAR γ partial agonists. *Bioorg Med Chem Lett* **15**:5035–5038.
- Elbrecht A, Chen Y, Adams A, Berger J, Griffin P, Klatt T, Zhang B, Menke J, Zhou G, Smith RG, et al. (1999) L-764406 is a partial agonist of human peroxisome proliferator-activated receptor γ . The role of Cys313 in ligand binding. *J Biol Chem* **274**:7913–7922.
- Fujimura T, Kimura C, Oe T, Takata Y, Sakuma H, Aramori I, and Mutoh S (2006) A selective peroxisome proliferator-activated receptor gamma modulator with distinct fat cell regulation properties. *J Pharmacol Exp Ther* **318**:863–871.
- Gampe RT Jr, Montana VG, Lambert MH, Miller AB, Bledsoe RK, Milburn MV, Kliewer SA, Willson TM, and Xu HE (2000) Asymmetry in the PPAR γ /RXR α crystal structure reveals the molecular basis of heterodimerization among nuclear receptors. *Mol Cell* **5**:545–555.
- Hunt CR, Ro JHS, Dobson DE, Min HY, and Spiegelman B (1986) Adipocyte P2 gene developmental expression and homology of 5'-flanking sequences among fat cell-specific genes. *Proc Natl Acad Sci U S A* **83**:3786–3790.
- Jiang HP and Serrero G (1992) Isolation and characterization of a full-length cDNA coding for an adipose differentiation-related protein. *Proc Natl Acad Sci U S A* **89**:7856–7860.
- Kintscher U, Goetze S, Wakino S, Kim S, Nagpal S, Chandraratna RA, Graf K, Fleck E, Hsueh WA, and Law RE (2000) Peroxisome proliferator-activated receptor and retinoid X receptor ligands inhibit monocyte chemotactic protein-1-directed migration of monocytes. *Eur J Pharmacol* **401**:259–270.
- Liu K, Black RM, Acton JJ 3rd, Mosley R, Debenham S, Abola R, Yang M, Tschirret-Guth R, Colwell L, Liu C, et al. (2005) Selective PPAR γ modulators with improved pharmacological profiles. *Bioorg Med Chem Lett* **15**:2437–2440.
- McRee DE (1999) XtalView/Xfit—A versatile program for manipulating atomic coordinates and electron density. *J Struct Biol* **125**:156–165.
- Miller CP (2002) SERMs: evolutionary chemistry, revolutionary biology. *Curr Pharm Des* **8**:2089–2111.
- Minoura H, Takeshita S, Ita M, Hirosumi J, Mabuchi M, Kawamura I, Nakajima S, Nakayama O, Kayakiri H, Oku T, et al. (2004) Pharmacological characteristics of a novel nonthiazolidinedione insulin sensitizer, FK614. *Eur J Pharmacol* **494**:273–281.
- Nolte RT, Wisely GB, Westin S, Cobb JE, Lambert MH, Kurokawa R, Rosenfeld MG, Willson TM, Glass CK, and Milburn MV (1998) Ligand binding and co-activator assembly of the peroxisome proliferator-activated receptor-gamma. *Nature* **395**:137–143.
- Oberfield JL, Collins JL, Holmes CP, Goreham DM, Cooper JP, Cobb JE, Lenhard JM, Hull-Ryde EA, Mohr CP, Blanchard SG, et al. (1999) A peroxisome proliferator-activated receptor gamma ligand inhibits adipocyte differentiation. *Proc Natl Acad Sci U S A* **96**:6102–6106.
- Ostberg T, Svensson S, Selen G, Uppenberg J, Thor M, Sundbom M, Sydow-Backman M, Gustavsson AL, and Jendeborg L (2004) A new class of peroxisome proliferator-activated receptor agonists with a novel binding epitope shows antidiabetic effects. *J Biol Chem* **279**:41124–41130.
- Otwinowski Z and Minor W (1997) Processing of X-ray diffraction data collected in oscillation mode. *Methods Enzymol* **276**:307–326.
- Sack JS (1988) CHAIN—a crystallographic modeling program. *J Mol Graph* **6**:224–235.

- Schupp M, Clemenz M, Gineste R, Witt H, Janke J, Helleboid S, Hennuyer N, Ruiz P, Unger T, Staels B, et al. (2005) Molecular characterization of new selective peroxisome proliferator-activated receptor gamma modulators with angiotensin receptor blocking activity. *Diabetes* **54**:3442–3452.
- Sheu SH, Kaya T, Waxman DJ, and Vajda S (2005) Exploring the binding site structure of the PPAR gamma ligand-binding domain by computational solvent mapping. *Biochemistry* **44**:1193–1209.
- Shi GQ, Dropinski JF, McKeever BM, Xu S, Becker JW, Berger JP, MacNaul KL, Elbrecht A, Zhou G, Doebber TW, et al. (2005) Design and synthesis of alpha-aryloxyphenylacetic acid derivatives: a novel class of PPARalpha/gamma dual

agonists with potent antihyperglycemic and lipid modulating activity. *J Med Chem* **48**:4457–4468.

- Tontonoz P, Hu E, Devine J, Geale EG, and Spiegelman BM (1995) PPAR γ 2 regulates adipose expression of the phosphoenolpyruvate carboxykinase gene. *Mol Cell Biol* **15**:351–357.

Address correspondence to: Dr. Joel P. Berger, RY80N-C31, Merck Research Laboratories, 126 E. Lincoln Ave., Rahway, NJ 07065. E-mail: joel_berger@merck.com
